Research
Watershed Ecology—Article

# A Comparison of SWAT Model Calibration Techniques for Hydrological Modeling in the Ganga River Watershed

Nikita Shivhare *, Prabhat Kumar Singh Dikshit, Shyam Bihari Dwivedi

*Indian Institute of Technology, Banaras Hindu University, Varanasi 221005, India*

## ARTICLE INFO

## ABSTRACT

The Ganga River, the longest river in India, is stressed by extreme anthropogenic activity and climate change, particularly in the Varanasi region. Anticipated climate changes and an expanding populace are expected to further impede the efficient use of water. In this study, hydrological modeling was applied to Soil and Water Assessment Tool (SWAT) modeling in the Ganga catchment, over a region of 15 621.612 km$^2$ in the southern part of Uttar Pradesh. The primary goals of this study are: ① To test the execution and applicability of the SWAT model in anticipating runoff and sediment yield; and ② to compare and determine the best calibration algorithm among three popular algorithms—sequential uncertainty fitting version 2 (SUFI-2), the generalized likelihood uncertainty estimation (GLUE), and parallel solution (ParaSol). The input data used in the SWAT were the Shuttle Radar Topography Mission (SRTM) digital elevation model (DEM), Landsat-8 satellite imagery, soil data, and daily meteorological data. The watershed of the study area was delineated into 46 sub-watersheds, and a land use/land cover (LULC) map and soil map were used to create hydrological response units (HRUs). Models utilizing SUFI-2, GLUE, and ParaSol methods were constructed, and these algorithms were compared based on five categories: their objective functions, the concepts used, their performances, the values of *P*-factors, and the values of *R*-factors. As a result, it was observed that SUFI-2 is a better performer than the other two algorithms for use in calibrating Indian watersheds, as this method requires fewer runs for a computational model and yields the best results among the three algorithms. ParaSol is the worst performer among the three algorithms. After calibrating using SUFI-2, five parameters including the effective channel hydraulic conductivity (CH_K2), the universal soil-loss equation (USLE) support parameter (USLE_P), Manning's *n* value for the main channel (CH_N2), the surface runoff lag time (SURLAG), and the available water capacity of the soil layer (SOL_AWC) were observed to be the most sensitive parameters for modeling the present watershed. It was also found that the maximum runoff occurred in sub-watershed number 40 (SW#40), while the maximum sediment yield was 50 t·a$^{-1}$ for SW#36, which comprised barren land. The average evapotranspiration for the basin was 411.55 mm·a$^{-1}$. The calibrated model can be utilized in future to facilitate investigation of the impacts of LULC, climate change, and soil erosion.

## 1. Introduction

In terms of the land and climate characteristics of the southern Uttar Pradesh Basin, tendencies toward sudden floods and soil erosion present some of the most extreme issues. Because of soil erosion, the soil of this watershed is continuously degrading and losing nutrients, thus affecting agriculture in the state. The severity of the issue is intensified in arid and semi-arid lands, where short-duration intense rainfall and unsustainable land use have quickened soil losses by erosion. Detailed and accurate information regarding soil erosion and surface water discharge is helpful for watershed managers to better manage and conserve natural resources such as soil and water, and to promote sustainable development. At present, various procedures are used for hydrological modeling, utilizing precipitation, land use, and soil characteristics information. Among these are the Water Evaluation and Planning (WEAP) system, Agricultural Non-Point Source Pollution (AGNPS) system, Areal Nonpoint Source Watershed Environment Response Simulation (ANSWERS), Soil and Water Assessment Tool (SWAT), and Water Erosion Prediction Project (WEPP). Among these strategies, the SWAT is a process-based hydrological model developed by the

* Corresponding author.
 *E-mail address:* nikitas.rs.civ15@iitbhu.ac.in (N. Shivhare).

United States Department of Agriculture (USDA) Agricultural Research Service (ARS) [1]. Additional algorithms have been developed to best estimate the parameters used in hydrological modeling.

The SWAT is widely used for hydrological and sediment yield modeling. It is a time-consistent and spatially appropriate test model that was developed to assist watershed managers in anticipating the effects of land use management activities on runoff, soil erosion, and agricultural chemical yields [2]. Specialists have effectively used the SWAT for runoff assessments [3,4], water quality modeling [5,6], hydrological and river basin modeling [7–9], sediment yield modeling [10–13], and the management of erosion-prone areas [1,14]. Psomas et al. [15] utilized the SWAT and WEAP to develop water efficiency measures in Greece.

To modify the elements that influence SWAT yields, calibration using observed values and evaluated estimations of runoff, evapotranspiration, and other SWAT outputs is necessary. Validation is a way that compares SWAT results with the observed data, without modifying the values of the influencing factors. Calibration of various parameters is necessary for proper hydrological modeling. There are 26 parameters distinguished for runoff, more than 30 for soil disintegration, and 41 for water quality, all of which can be utilized for calibration. The calibration of such a circulated parameterized watershed model entails some significant issues that require careful attention on the part of investigators, particularly in regard to uncertainty [9]. Qiu and Wang [5] performed validation and calibration for the periods 1997–2002 and 2003–2008, respectively, for the hydrological and water quality evaluation of central New Jersey. Vigiak et al. [16] performed calibration and validation for hillslope erosion modeling of the Danube Basin.

Earlier researchers applied deterministic approaches such as the trial and error method for uncertainty analysis, calibration, and validation. When using such methods, it is necessary to continue to alter the parameters until a sensible match is achieved between the simulation and observations. However, these approaches are now outdated; scientists have developed many stochastic algorithms for calibration, validation, and uncertainty analysis. Some of the widely used algorithms for calibration are sequential uncertainty fitting version 2 (SUFI-2), parallel solution (ParaSol), particle swarm optimization (PSO), generalized likelihood uncertainty estimation (GLUE), artificial neural network (ANN), and Markov chain Monte Carlo (MCMC).

Vilaysane et al. [17] used the SUFI-2 technique to calibrate the values for hydrological stream flow modeling of the Xedone River Basin. Yesuf et al. [12] utilized SUFI-2 and SWAT-CUP for sediment yield modeling in Ethiopia; they reported that SUFI-2 utilized a computerized advancement system that was equipped to perform affectability, alignment, approval, and vulnerability examinations with enhanced model run time proficiency. Ercan et al. [18] used cloud techniques for SWAT model calibration. Talebizadeh et al. [19] used ANN and the SWAT for sediment load modeling and uncertainty analysis. Calibration and validation have also been done using genetic algorithms and Bayesian model averaging [20]. Tuo et al. [21] applied the SUFI-2 algorithm for uncertainty analysis when evaluating precipitation input for the SWAT model. Noori and Kalin [4] coupled ANN with the SWAT and SWAT-CUP for daily streamflow prediction. Similarly, runoff [3] and sediment fluxes modeling [13] have been done using the SUFI-2 algorithm. An approximation of the SWAT model can also be constructed using ANN and a support vector machine (SVM) [22]. Out of all these algorithms, it is difficult to determine the best algorithm for the calibration of SWAT outputs. Therefore, in the present study, we consider the three calibration-uncertainty analysis algorithms of GLUE, SUFI-2, and ParaSol.

In the present study, SWAT 2012 was used for hydrological modeling. For calibration, the three widely used algorithms of GLUE, SUFI-2, and ParaSol were applied and compared in order to determine the best calibration technique. In this investigation, the ArcSWAT Interface was associated with the Ganga River Basin for depicting and organizing sub-watersheds in order to gauge and model runoff, sediment yield, and evapotranspiration. The model required a digital elevation model (DEM), a land use/land cover (LULC) map, and a soil map as inputs for watershed delineation and hydrological response unit (HRU) analysis. Daily meteorological data from the four stations of Balia, Varanasi, Babatpur, and Gazipur were utilized from 1996 to 2015. The major target of this examination was to delineate the watersheds, divide the study area into sub-watersheds, determine the number of streams, and estimate their order, and then to establish information regarding the outlet points and reservoirs available in the watershed in order to accurately divide it into HRUs having similar but unique land types, soil types, and elevation properties. These units permit simpler modeling. Finally, after providing the meteorological data, the SWAT was run to estimate runoff, sediment yield, and evapotranspiration for each HRU and sub-watershed. The model was then calibrated for the observed data from the years 2004–2009 at the sub-watershed and watershed level using the SUFI-2, GLUE, and ParaSol algorithms. By analyzing the results, assumptions, and limitations of these calibration techniques, the best technique among the three was determined based on five categories, as described in Section 4.2. The model calibrated using the best technique was then validated for the period of 2009–2015. Finally, the estimated and corrected results of the hydrological parameters were calculated, and modeling was conducted.

## 2. Study area

The study area for which modeling was performed in the present study is part of the Ganga River Basin that occupies the southern of Uttar Pradesh State of India. The length of the river in this watershed is about 50 km, and the total area of the watershed is 15 621.612 km². The area lies between latitude 82°1′52.439″ E to 83°55′10.63 E and longitude 26°2′7.842″ N to 24°22′53.034″ N. The major stations covered by the study area are the Varanasi, Balia, Babatpur, Gazipur, Mirzapur, and Chandauli Districts. The mainstream flow of the study area lies in the Varanasi District. The average rainfall in this area is 941.2 mm, with the maximum rainfall occurring in July, August, and September and the minimum rainfall occurring in June and October. From November to May, the study area receives negligible rainfall. This part of the basin is barren, and urban lands cover more than 50% of the basin.

## 3. Data

Elevation data, LULC data, soil data, and daily meteorological data were the prerequisites for the present modeling. The Shuttle Radar Topology Mission (SRTM) DEM, with a resolution of 90 m × 90 m, was used for elevation data. For the LULC map, image classification was performed using satellite imagery from Landsat 8. For meteorological input, data for the daily rainfall, temperature, solar radiation, and pressure for 20 years were used. Detailed information on the data used and on their locations, periods, and the organizations from which they were procured is given in Table 1.

## 4. Methods and procedures

### 4.1. Soil and Water Assessment Tool (SWAT)

In this study, SWAT 2012 was utilized for hydrological modeling. ArcGIS 10 software was used along with its extension, ArcSWAT. The catchment was split into various sub-catchments,

**Table 1**
Details of the raw data used for modeling.

| Data | Location | Period of record | Organization | Primary use |
|---|---|---|---|---|
| STRM DEM | 82°1′52.439″ E 26°2′7.842″ N to 83°55′10.63″ E 24°22′53.034″ N | — | USGS | Watershed delineation |
| Satellite imagery (Landsat 8) | 82°1′52.439″ E 26°2′7.842″ N to 83°55′10.63″ E 24°22′53.034″ N | November 2014 | USGS | To create LULC map and model input |
| Soil data | Uttar Pradesh | — | NBSSLUP | To create soil map and model input |
| Climate data | Varanasi, Balia, Babatpur, and Gazipur | 1996–2015 | IMD Pune | Model input |

IMD: Indian Meteorological Department; USGS: United States Geological Survey; NBSSLUP: the National Bureau of Soil Survey and Land Use Planning.

which were then further categorized into HRUs. Each HRU comprises a unique combination of soil characteristics, elevation, and LULC. The water budget was the primary impetus behind all forms, and the HRU was the unit used to estimate the hydrologic parameters. These procedures were separated into two stages: ① A land stage, wherein the SWAT mimics the catchment loadings of the stream, residue, and supplements from each HRU, which are then locale-weighted to the sub-basin level; and ② an in-stream stage, wherein the model tracks the course of the catchment loadings from each sub-basin throughout the channel organization.

A solitary plant-improvement model was utilized as a part of the SWAT in order to reenact extraordinary land-cover types including expansive information yield. This development model was utilized to evaluate the expulsion of water and supplements from the root zone, transpiration, and biomass generation. Planting, reaping, culturing passes, and supplement and pesticide applications could be recreated for each trimming framework with particular dates [23]. Once the data for each HRU were determined at the sub-basin level, the runoff, sediments, nutrients, and pesticides were routed through channels, ponds, reservoirs, and wetlands to the watershed outlet.

The SWAT theoretical documentation version 2009 by Neitsch et al. [24] can be used as a reference to learn more about SWAT modeling.

### 4.2. Sequential uncertainty fitting version 2 (SUFI-2)

The SUFI-2 technique is a stochastic algorithmic approach that is most frequently used by scientists to evaluate uncertainty. In this algorithm, the extent to which all uncertainties are represented is assessed by a parameter referred to as the *P*-factor. This parameter is the percentage of estimated information sectioned by the 95% prediction uncertainty, which is also called the 95PPU. Another parameter evaluating the quality of the calibration is the *R*-factor, which is the standard thickness of the 95PPU band separated by the standard deviation of the predetermined information. Hypothetically, the estimation of the *P*-factor ranges from 0 to 100%, while that of the *R*-factor ranges from 0 without limit. A *P*-factor of 1 and an *R*-factor of 0 signify a recreation that precisely compares with the predetermined information. In this study, SWAT-CUP was the software used to consolidate the SWAT 2012 simulated values with the observed values. Using these values and the SUFI-2 algorithm, the uncertainty analysis and calibration were performed.

A short well-ordered depiction of the SUFI-2 algorithm is as follows:

**Step 1:** The objective function ($g_i$) is characterized. Next, the minimum and maximum absolute ranges ($\theta_j$) of the physically important parameters being optimized are identified.

**Step 2:** A sensitivity analysis for each of the parameters is completed; afterward, the initial uncertainty ranges are relegated to the parameters for the first round of Latin hypercube testing.

**Step 3:** Latin hypercube sampling is performed, and the corresponding objective functions are assessed. The sensitivity matrix

$J_{ij}$ and the parameter covariance grid $C$ are calculated by the following:

$$J_{ij} = \frac{\Delta g_i}{\Delta \theta_j}, \quad i = 1, 2, \dots, C_m, \quad j = 1, 2, \dots, p \quad (1)$$

where $C_m$ is the number of rows in the sensitivity matrix, and $p$ is the number of parameters to be estimated.

$$C = S_g^2 (J^T J)^{-1} \quad (2)$$

where $S_g^2$ is the variance of the objective function values resulting from the $m$ model runs.

**Step 4:** The 95PPU is then calculated, followed by the *P*-factor and *R*-factor.

### 4.3. Generalized likelihood uncertainty estimation (GLUE)

The GLUE was applied in order to consider the non-uniqueness of the parameter sets during the estimation of model parameters in over-parameterized models. This method is simple; for vastly over-parameterized models, GLUE accepts that there is no unusual arrangement of parameters that optimizes the decency-of-fit criteria. In GLUE, all sources of parameter uncertainties are considered in the parameter uncertainty. The probability esteem, which is related to a parameter set, mirrors all sources of error and the impacts of covariation of parameter esteem on the model execution. A GLUE examination comprises the following three stages:

(1) After defining the "generalized likelihood measure," $L(\phi)$, many parameter sets are randomly sampled from the earlier dissemination; each parameter set is assessed as either "behavioral" or "non-behavioral" through a comparison of the "likelihood measure" with a selected threshold value.

(2) Each behavioral parameter set is given a "likelihood weight", $W_i$, according to the following:

$$W_i = L(\phi_i) \bigg/ \sum_{k=1}^{n} L(\phi_k) \quad (3)$$

where $n$ is the number of behavioral parameter sets.

(3) Finally, the prediction uncertainty is depicted as a forecast quintile from the aggregate dissemination acknowledged from the weighted behavioral parameter sets. The most frequently utilized likelihood measure for GLUE is the Nash-Sutcliffe coefficient of efficiency (NSE).

### 4.4. Parallel solution (ParaSol)

ParaSol depends on an adjustment to the worldwide optimization calculation, SCE-UA. The motivation is to utilize the simulation performed during optimization to derive prediction uncertainty. The simulations accumulated by SCE-UA are extremely important, as the calculation tests over the whole parameter space with an emphasis on arrangements close to the ideal/optima.

The process of ParaSol is as follows:

(1) After streamlining the application of the changed SCE-UA (the arbitrariness of the SCE-UA calculation is expanded to enhance

the scope of the parameter space), the reproductions performed are partitioned into "great" recreations and "not great" recreations using a limit estimation of the target work, as in GLUE. This yields "great" parameter sets and "not great" parameter sets.

(2) A prediction of uncertainty is built by similarly weighing every "great" recreation. The target work utilized as a part of ParaSol is the sum of the squares of the residuals (SSQ):

$$\text{SSQ} = \sum_{i=1}^{n} \left( y_{i,\text{M}}(\phi) - y_{i,\text{S}} \right)^2 \tag{4}$$

where $n$ is the number of measured variables, $y_{i,\text{M}}(\phi)$, and simulated variables, $y_{i,\text{S}}$.

Brief descriptions of the SWAT-CUP, SUFI-2, GLUE, and ParaSol model components are found in the SWAT-CUP user manual by Abbaspour [25] and in the SWAT model use, calibration, and validation document by Arnold et al. [26].

### 4.5. Data pre-processing

The input data required for SWAT modeling are DEM, a LULC map, a soil map, and meteorological data. First, the raw data procured from the different organizations described in Table 1 were pre-processed. The different DEMs downloaded from the United States Geological Survey (USGS) were mosaicked using the mosaicking tool in ArcGIS 10. In the mosaicking tool, multiple images are joined into one unit. To obtain a LULC map, the satellite imagery was processed. Image classification was performed using the ERDAS Imagine tool. Any satellite image comprises multiple bands in the electromagnetic spectrum. All the bands together form an image; however, this provides only spectral information. Converting the spectral information into LULC information classes or into any other particular information class requires image classification. Information classes are categorical classes, in which a pixel may represent a water area, forested area, or urban area. Based on a spectral curve or the spectrum of the pixel, classification is possible. There are two types of automated image classification techniques: supervised and unsupervised digital image classification. In supervised digital image classification, the software is guided by researchers or image interpreters with expertise in specifying the land cover classes of interest as a signature dataset, which is then automatically used by the software to create spectral classes. In unsupervised digital image classification, an interpreter only specifies the number of classes required to classify the image; the system then classifies the image without researchers' expertise. The LULC map of this region (Fig. 1) was extracted by performing supervised classification on the optical satellite imagery. A signature dataset was created for six classes—water (WATR), forested areas (FRSD), urban areas (URBN), range (RNGE), agriculture (AGRL), and barren land (BARR)—using the visual interpretation keys; approximately 150 training datasets were used for a single class. The classification algorithm that was used was maximum likelihood. Most of the watershed comprises urban or barren land.

To construct the soil map shown in Fig. 2, soil data were collected using National Bureau of Soil Survey and Land Utilisation Planning (NBSS & LUP) data and laboratory test results. The soil was divided into five layers. A user soil database describing each soil class was constructed for use in HRU analysis, as shown in Table 2. A climate database was created using Indian Meteorological Department (IMD) data; the latitude and longitude were given along with the rainfall, temperature, and solar radiation data in separate text files.

### 4.6. SWAT modeling

The watershed is defined to include both the catchment and the drainage channel within a single morphometric divide. It is a nat-
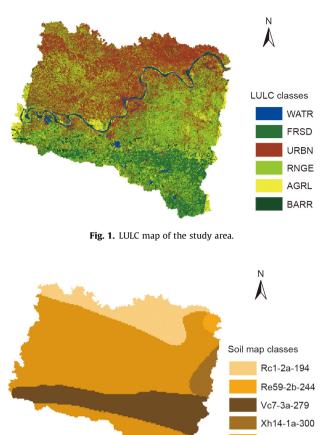


**Fig. 1.** LULC map of the study area.



**Fig. 2.** Soil map of the study area.

urally occurring hydrologic unit that is covered by natural boundaries and characterized by similar conditions such as physical characteristics, the topology of the land surface, and climatic conditions. Watershed delineation implies the drawing of lines on a map to indicate a watershed's limits; these are commonly drawn on maps utilizing data from DEM or contour maps.

Watershed delineation is the first step of SWAT modeling. DEM is used as the input in this step. Along with the slope of the watershed, the streams and outlet points are generated. According to the outlet points selected by the researcher, the watershed is delineated. The user can also provide data related to the reservoir and predefined streams as input. In this project, the watershed was delineated by dividing the watershed into 46 sub-watersheds. Fig. 3 shows the delineated watershed, streams, and monitoring points of the study area. The next step is the HRU analysis. In HRU analysis, the watershed is divided into units having similar but unique land types, soil types, and elevation properties. In this step, using the soil map, user soil table, LULC map, and slope map (Fig. 4) of the study area, the watershed was divided into 160 HRUs. In the next step, the climate database was provided to the model. Finally, the SWAT model was run to yield the runoff, evapotranspiration, and sediment yields of each sub-watershed and HRU for 20 years.

### 4.7. Calibration and validation

As noted earlier, calibration is the modification of the elements influencing the SWAT yields, and is assisted by observed values and evaluated estimations of runoff, evapotranspiration, and other

**Table 2**
Details of user soil table.

| | SNAM (Soil properties) | Soil classes | | | | |
|---|---|---|---|---|---|---|
| | | Rc1-2a-194 | Re59-2b-244 | Vc7-3a-279 | Xh14-1a-300 | Xh14-ab-303 |
| General | S5ID | IND194 | IND244 | IND279 | IND300 | IND303 |
| | HYDGRP (hydrological soil group)[a] | D | C | D | C | C |
| | TEXTURE[b] | L | L | CL | SCL | SL |
| Layer 1 | SOL_Z1 (depth of soil in mm) | 300 | 300 | 300 | 300 | 300 |
| | SOL_BD1 (bulk density in $gm \cdot mL^{-1}$) | 1.5079 | 1.5583 | 1.5043 | 1.5847 | 1.5952 |
| | SOL_AWC1 (available water capacity in mm $H_2O$ per mm soil) | 0.1441 | 0.1192 | 0.1327 | 0.0984 | 0.0893 |
| | SOL_K1 (hydraulic conductivity in $mm \cdot h^{-1}$) | 4.1604 | 9.7772 | 4.0563 | 12.9805 | 30.1535 |
| | SOL_CBN1 (carbon content in percentage of soil weight) | 0.6% | 0.8% | 0.8% | 0.7% | 0.6% |
| | CLAY1 (percentage of clay) | 28% | 22% | 30% | 21% | 13% |
| | SILT1 (percentage of silt) | 43% | 31% | 34% | 21% | 23% |
| | SAND1 (percentage of sand) | 30% | 47% | 36% | 58% | 64% |
| | SOL_ALB1 (soil albedo)[c] | 0.3971 | 0.346 | 0.346 | 0.3707 | 0.3971 |
| | USLE_K1 (USLE erodibility factor) | 0.1719 | 0.163 | 0.1589 | 0.1569 | 0.1687 |
| Layer 2 | SOL_BD2 (bulk density in $gm \cdot mL^{-1}$) | 1.535 | 1.5561 | 1.4814 | 1.5972 | 1.6026 |
| | SOL_AWC2 (available water capacity n mm $H_2O$ per mm soil) | 0.1202 | 0.1158 | 0.1387 | 0.0957 | 0.0914 |
| | SOL_K2 (hydraulic conductivity in $mm \cdot h^{-1}$) | 3.6147 | 10.3717 | 2.4191 | 12.8314 | 21.7927 |
| | SOL_CBN2 (carbon content in percentage of soil weight) | 0.5% | 0.9% | 0.4% | 0.5% | 0.5% |
| | CLAY2 (percentage of clay) | 31% | 22% | 34% | 21% | 16% |
| | SILT2 (percentage of silt) | 26% | 28% | 36% | 20% | 22% |
| | SAND2 (percentage of sand) | 43% | 49% | 29% | 59% | 62% |
| | SOL_ALB2 (soil albedo) | 0.4254 | 0.323 | 0.4557 | 0.4254 | 0.4254 |
| | USLE_K2 (USLE erodibility factor) | 0.1561 | 0.158 | 0.1647 | 0.1583 | 0.1658 |

[a] Hydrological soil groups are of four types: Type A, having an infiltration rate of 7.6–11.4 $mm \cdot h^{-1}$; Type B, having an infiltration rate of 3.8–7.6 $mm \cdot h^{-1}$; Type C, having an infiltration rate of 1.3–3.8 $mm \cdot h^{-1}$; and Type D, having infiltration rate of 0–1.3 $mm \cdot h^{-1}$.
[b] Texture L: loamy; CL: clay loamy; SCL: silty clay loamy; SL: silty loamy.
[c] Soil ALB is the soil albedo: ratio of amount of solar radiation reflected by a body to the amount incident upon it.
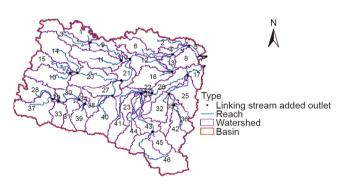


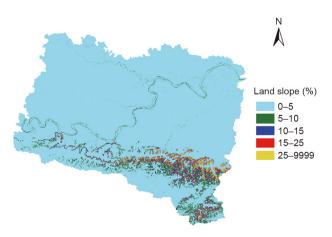**Fig. 3.** Watershed delineation of the study area.



**Fig. 4.** Slope map of the study area.

SWAT outputs. Validation compares the SWAT results with the observed data without modifying the values of the influencing factors. Calibration is necessary for proper hydrological modeling. There are 34 parameters distinguished for runoff and soil erosion

**Table 3**
Parameters used for calibration, with their absolute ranges.

| Parameters | Description | Minimum | Maximum |
|---|---|---|---|
| GW_DELAY | Groundwater delay (d) | 0 | 500 |
| OV_N | Manning's $n$ value for overland flow | 0.01 | 30 |
| SOL_K | Saturated hydraulic conductivity | 0 | 2000 |
| ALPHA_BF | Base flow alpha factor | 0 | 1 |
| CH_N2 | Manning's $n$ value for the main channel | −0.01 | 0.3 |
| CH_K2 | Effective hydraulic conductivity in main channel alluvium | −0.01 | 500 |
| CN2 | SCS runoff curve number $f$ | 35 | 98 |
| USLE_P | USLE equation support parameter | 0 | 1 |
| SOL_AWC | Available water capacity of the soil layer | 0 | 1 |
| SURLAG | Surface runoff lag time | 0.05 | 24 |
| USLE_K | USLE equation soil erodibility ($K$) factor | 0 | 0.65 |

SCS: soil conservation service; USLE: universal soil loss equation.

that can be utilized for calibration. Table 3 describes the parameters used in the present study for calibration, along with their minimum and maximum absolute SWAT values. In this step, SWAT-CUP was used as an interface between the SWAT and calibration algorithms to perform the uncertainty analysis, calibration, and validation of the hydrological modeling outputs. The TxtInOut folder of the SWAT model was imported into the SWAT-CUP software for input. The observed values of surface water discharge of the Varanasi sub-watershed were calculated using the acoustic Doppler current profiler (ACDP) for the years 1996–2015. These values were used for comparison and calibration. The input files of the SWAT-CUP model were updated as necessary. Fig. 5 shows the detailed procedure as a flowchart.

### 4.8. Methodology and criteria for comparison

Different challenges appear when comparing calibration techniques used for soil and water modeling. The most important
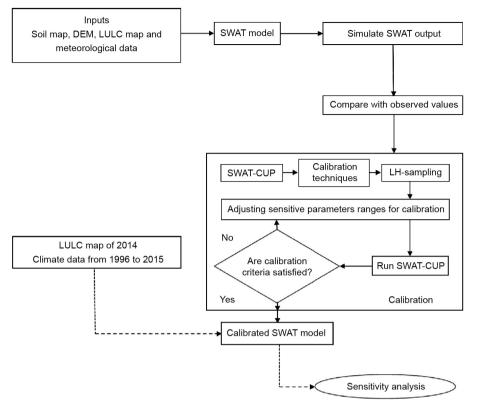
**Fig. 5.** Calibration flowchart.

concerns that we addressed while comparing these techniques are as follows:

(1) Most algorithms are diverse in their theories. Subjective decisions must be made in their formulation concerning prior parameter distributions and objective functions. In this study, we addressed this issue by choosing objective functions for each algorithm as they would be utilized in hydrological applications. Fundamentally, this leads to various objective functions for various algorithms. In discussing the outcomes, we indicate whether an issue is caused by the theoretical definition of a specific algorithm or by the choice of the function.

(2) Every algorithm has its own fundamental concept and objective functions, which impairs comparison. To solve this problem, the value of each function behind every algorithm was calculated to permit fair comparison. Similarly, we utilized the measures of computational proficiency and an appraisal of the conceptual basis criteria for better comparison.

(3) It is fairly obvious that each algorithm yields different results. To address this problem, we considered the results of all the algorithms for all possible criteria; we then outlined them all so that the reader can draw his or her own particular conclusions.

(4) The outcomes of the comparison innately depend upon the applications. To solve this issue, the specific results of each application of the algorithm are separated from the generic ones.

The following five categories were used for the comparison of the three (SUFI-2, GLUE, and ParaSol) calibration algorithms: The calibration techniques use several parameters for calibration. For each technique, the best estimate and uncertainty range of these parameters differ, so the first comparison is based on the best estimate, the minimum and maximum uncertainty ranges of each algorithm, and the parameter correlation. The various algorithms use various objective functions, so the second comparison is based on the values of NSE, $R^2$, and other objective functions. The third comparison is based on the values of the $R$-factor, which is the average width of the

band divided by the standard deviation of the corresponding measured variable, and on the $P$-factor, which is the percentage of data bracketed by the 95PPU band of each algorithm. The fourth comparison was based on theoretical concepts, testability, and the fulfillment of statistical assumptions. The final comparison was based on the difficulty of implementation.

## 5. Results

### 5.1. SWAT output

In the present study, the SWAT model was run for a watershed located in the northern part of India in the state of Uttar Pradesh. The SWAT divided the watershed into 46 sub-watersheds and 760 HRUs for easy and accurate modeling. It was estimated that the average annual precipitation of the basin is 941.24 mm, snowfall is 0 mm, snowmelt is 0 m, surface runoff (SUR Q) is 358.56 mm, lateral discharge is 1.39 mm, and groundwater discharge for shallow and deep aquifers is 138.69 and 8.53 mm, respectively. The average value for total aquifer recharge is 180.65 mm, the total water yield of the basin is 507.17 mm, and evapotranspiration is 411.7 mm. A pictorial representation of the SWAT output regarding runoff and evapotranspiration is shown in Fig. 6. The results indicated that, on average, more than 45% of the total precipitated water is lost in runoff and evapotranspiration. The average monthly values of all the parameters of the basin—that is, rainfall, snowfall, surface runoff, lateral runoff, water yield, and evapotranspiration—are given in Table 4. It was also estimated that there are an average of 52.11 annual water-stress days and 10.54 temperature-stress days.

During watershed image classification, the watershed was classified into six classes according to the land use. It was found that most of the watershed is urban or barren land. Table 5 gives the
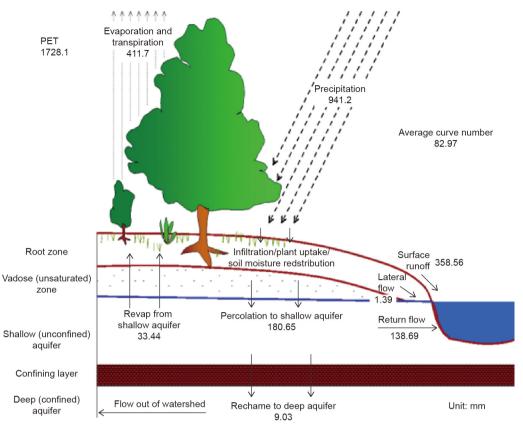
**Fig. 6.** Pictorial representation of the SWAT output.

**Table 4**
Average monthly values of the parameters for the watershed.

| Month | Rainfall (mm) | Snowfall (mm) | SUR Q (mm) | Lateral Q (mm) | Water yield (mm) | ET (mm) | SED (t·hm$^{-2}$) | PET (mm) |
|---|---|---|---|---|---|---|---|---|
| Jan | 16.30 | 0 | 3.11 | 0.03 | 4.29 | 13.75 | 0.08 | 84.90 |
| Feb | 15.60 | 0 | 2.07 | 0.03 | 2.77 | 16.56 | 0.05 | 94.98 |
| Mar | 4.09 | 0 | 0.40 | 0.02 | 0.91 | 42.98 | 0.01 | 186.43 |
| Apr | 5.14 | 0 | 0.38 | 0.02 | 0.67 | 27.98 | 0.01 | 211.08 |
| May | 13.41 | 0 | 0.97 | 0.02 | 1.17 | 16.06 | 0.01 | 214.76 |
| Jun | 107.36 | 0 | 22.41 | 0.05 | 19.80 | 34.62 | 0.29 | 190.49 |
| Jul | 255.36 | 0 | 103.17 | 0.21 | 103.50 | 68.92 | 1.18 | 134.00 |
| Aug | 274.62 | 0 | 115.85 | 0.32 | 136.90 | 72.31 | 2.11 | 122.88 |
| Sep | 201.68 | 0 | 94.99 | 0.34 | 145.24 | 59.26 | 2.14 | 123.88 |
| Oct | 28.68 | 0 | 9.61 | 0.20 | 56.11 | 32.92 | 0.19 | 151.62 |
| Nov | 8.89 | 0 | 2.33 | 0.10 | 25.71 | 15.84 | 0.07 | 121.75 |
| Dec | 10.00 | 0 | 3.26 | 0.06 | 10.09 | 10.35 | 0.06 | 90.63 |

Q: discharge or runoff; ET: evapotranspiration; PET: potential evapotranspiration; SED: sediment yield.

**Table 5**
Average annual values of the parameters for each land type.

| LULC type | Area (km$^2$) | CN | AWC (mm) | USLE_LS | Precipitation (mm) | SUR Q (mm) | GW Q (mm) | ET (mm) | SED (t·hm$^{-2}$) |
|---|---|---|---|---|---|---|---|---|---|
| WATR | 414.83 | 92.00 | 104.91 | 0.67 | 938.86 | 0 | 0 | 1374.49 | 0 |
| URBN | 5683.33 | 83.21 | 102.13 | 0.18 | 917.93 | 422.43 | 84.19 | 370.26 | 3.45 |
| RNGE | 5233.71 | 80.43 | 103.27 | 0.26 | 936.31 | 294.35 | 200.57 | 393.79 | 4.71 |
| AGRL | 1071.01 | 84.28 | 105.53 | 0.48 | 959.55 | 360.58 | 164.57 | 388.93 | 11.92 |
| BARR | 1268.02 | 92.10 | 106.89 | 0.31 | 947.23 | 556.68 | 33.29 | 327.52 | 29.27 |
| FRSD | 1948.26 | 80.64 | 118.56 | 0.98 | 1008.96 | 291.12 | 226.44 | 442.55 | 1.38 |

AWC: available water content capacity; CN: curve number; GW Q: groundwater discharge; USLE_LS: universal soil loss equation slope length factor.

annual average values of the parameters according to each land use type. It was also concluded from the results that for urban land, surface runoff may be excessive, and less than 22% of the water yield is base flow. For range and agricultural land, surface runoff may be excessive. For barren land, the sediment yield may be overly high, more than half of the precipitation is lost to runoff, the surface runoff is the highest, and less than 22% of the water yield is base flow.

Sediment loss from the landscape is dependent upon many factors. Sediment overestimation in SWAT usually arises from inadequate biomass production; this often occurs with specific land uses. SWAT also modifies sediments to consider in-stream deposition and the erosion of stream banks and channels. Often, little or no measured data are available to differentiate between upland sediment and in-stream sediment changes. Streams may be either net sources or sinks for sediment. In-stream sediment modification is impacted by the physical channel characteristics (i.e., slope, width, depth, channel cover, and substrate characteristics) and the quantity of sediment and flow from upstream. As a result, it was estimated that the maximum sediment yield is higher than 50 t·hm$^{-2}$ in at least one HRU. The highest value is from HRU #473, sub-basin #36, which is barren land with Vc7-3a-2 soil. It was also estimated that the total sediment load of the basin is 6.198 t·hm$^{-2}$.

A pictorial representation of the SWAT output regarding sediment yield is shown in Fig. 7. It was concluded from the results that the average upland sediment yield is 6.2 Mg·hm$^{-2}$ and the maximum upland sediment yield is 827.43 Mg·hm$^{-2}$.

### 5.2. Comparison output

Table 6 summarizes the comparison of the calibration algorithms. The comparison was performed over the five categories described earlier, with the following results:

**Category 1**: According to this category, GLUE is better than SUFI-2 and ParaSol, as GLUE has the widest range of uncertainties. Thus, most of the intervals considered by SUFI-2 and ParaSol are covered by GLUE. In this category, SUFI-2 is the second best.

**Category 2**: According to this category, ParaSol is the best for its objective function, that is, NSE, as it is based on a global optimization algorithm. As shown by the table values, it can be concluded that SUFI-2 and GLUE have similar values, so they hold the same position.

**Category 3**: According to this category, ParaSol is worse than the other two algorithms because of its narrow prediction uncertainty bands. From the other values, it can be concluded that SUFI-2 works better than GLUE.

**Category 4**: According to this category, all sources of uncertainties are considered by SUFI-2 and GLUE, whereas ParaSol only considers parameter uncertainty and ignores all other uncertainties. On a conceptual basis, SUFI-2 is better than GLUE and ParaSol because it gives the most efficient results.

**Category 5**: According to this category, GLUE is the best, as it is the easiest of the three algorithms.

From the comparison and description given in Section 5.2, we can conclude that the performances of SUFI-2 and GLUE are very similar. However, by looking at the 95PPU plot (Figs. 8 and 9), we concluded that SUFI-2 performs better than GLUE, as the results are more efficient and the algorithm considers uncertainties better. SUFI-2 can be run with the smallest number of parameters. GLUE works with a large number of simulations, but cannot provide better results than SUFI-2. The main drawback of GLUE is the length of the computational techniques because of its random sampling strategy. Thus, SUFI-2 is considered to be the best for this study, and further analysis of sediment yield calibration and validation was done using only the SUFI-2 algorithm.

### 5.3. SUFI-2 output

In the present analysis, the model was calibrated using the sensitive parameters given in Table 3. As indicated by the execution evaluation criteria of the model, which is suggested for a month-to-month time cycle, five parameters were determined to be the most sensitive parameters for modeling the present watershed. These parameters are the effective channel hydraulic conductivity (CH_K2), universal soil-loss equation (USLE), support parameter (USLE_P), Manning's $n$ value for the main channel (CH_N2), surface runoff lag time (SURLAG), and available water capacity of the soil layer (SOL_AWC). The behavioral threshold for calibration was
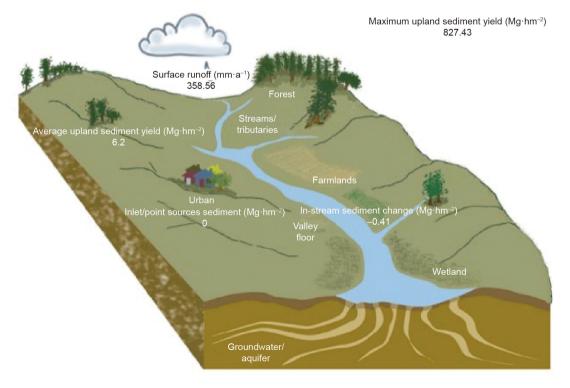


**Fig. 7.** SWAT output for sediment yield.

**Table 6**
Comparison of calibration algorithms, according to the criteria given in Section 4.8.

| Category | Criteria | GLUE | Parasol | SUFI-2 |
|---|---|---|---|---|
| 1[a] | GW_DELAY | 160.08 (9.52, 279.29) | 108.70 (92.23, 114.20) | 191.07 (100.04, 300.00) |
| | SOL_K | 0.16 (0.36, 0.78) | 0.37 (0.41, 0.34) | 0.10 (0.58, 0.34) |
| | ALPHA_BF | 0.12 (0.06, 0.97) | 0.12 (0.08, 0.13) | 0.51 (0.23, 0.74) |
| | OV_N | 0.05 (0.00, 0.20) | 0.11 (0.07, 0.10) | 0.06 (0.00, 0.11) |
| | CH_N2 | 0.30 (−0.01, 0.30) | 0.20 (0, 0.30) | 0.20 (0, 0.30) |
| | CH_K2 | 78.19 (6.01, 144.82) | 35.70 (27.72, 37.67) | 83.95 (69.42, 150.00) |
| | CN2 | 17.68 (28.85, 8.90) | 21.17 (20.93, 20.08) | 27.00 (29.00, 7.23) |
| | USLE_P | 0.40 (0, 1) | 0.50 (0, 1) | 0.30 (0, 1) |
| | SOL_AWC | 0.11 (0.01, 0.15) | 0.07 (0.08, 0.08) | 0.07 (0.05, 0.15) |
| | SURLAG | 2.00 (0.05, 24) | 3.20 (2.00, 20) | 2.00 (0.05, 23) |
| | USLE_K | 0.17 (0.01, 0.64) | 0.19 (0.07, 0.60) | 0.17 (0.01, 0.63) |
| | Parameter correlations | Yes | Yes | No |
| 2[b] | NSE | 0.76 | 0.77 | 0.76 |
| | $R^2$ | 0.77 | 0.66 | 0.78 |
| | $bR^2$ | 0.63 | 0.62 | 0.62 |
| 3 | P-factor | 0.76 | 0.18 | 0.79 |
| | R-factor | 0.65 | 0.08 | 1.51 |
| 4[c] | Source of parameter uncertainty | All sources | Parameter only | All sources |
| | Conceptual basis of parameter uncertainty | i. Normalization of generalized likelihood measure ii. Primitive random sampling strategy | i. Least squares (probability theory) ii. SCE-UA based sampling strategy | i Generalized objective function ii. Latin hypercube sampling; restriction of sampling intervals |
| | Testability of statistical assumption | No | Yes | Yes |
| 5 | Difficulty of implementation | Very easy | Easy | Easy |

[a] Best estimate values of parameters and their minimum and maximum range.
[b] Values of objective functions.
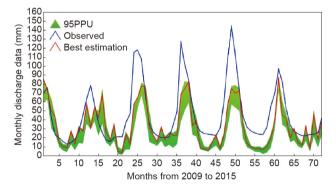[c] Uncertainty described by parameter uncertainty.



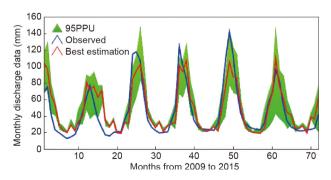**Fig. 8.** Plot of estimated and observed values after calibration using GLUE.



**Fig. 9.** Plot of estimated and observed values after calibration using SUFI-2.



**Fig. 10.** Plot of estimated and observed values of sediment yield (mm).

set to 0.500000. The period from 2000 to 2004 was considered to be a warm-up period. Data from the period 2004–2009 were used for calibration, and the data period 2009–2015 was used for validation. The results of the calibration and validation performed by the SUFI-2 algorithm are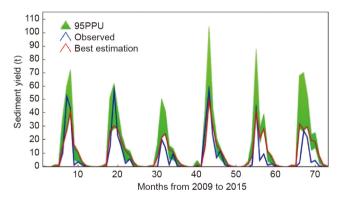 shown in Figs. 9 and 10. Fig. 9 shows a plot of the estimated and observed values of discharge and Fig. 10 shows a plot of the estimated and observed values of sediment data after calibration. Estimated outputs were compared at the same outlet point in sub-basin #27.

Table 7 lists the evaluation coefficients of the simulated monthly sediment yield of different objective functions for the study watershed. The assessment coefficients of the simulated month-to-month sediment yield of various target functions for the study area are recorded in Table 6. The P-factor, or the percentage of observations bracketed by the 95PPU, was 0.69. The R-factor was 0.763. The outcomes demonstrated that SUFI-2 sectioned a lower percentage of the observed sediment yield. Similarly, $R^2 = 0.78$, NSE = 0.76, percent bias (PBIAS) = $2.4 \times 10^2$, and the observation standard deviation ratio (RSR) = 0.49 are not strong indicators of the goodness of fit; however, they are within adequate evaluation ratings. The outcomes demonstrate that the SWAT can simulate the hydrological attributes of the Indian watershed extremely well. Hence, this model can be used for further hydrological studies in the basin.

**Table 7**
Objective function values.

| Method | P-factor | R-factor | $R^2$ | NSE | $bR^2$ | PBIAS | KGE | RSR |
|---|---|---|---|---|---|---|---|---|
| SUFI-2 | 0.69 | 0.763 | 0.78 | 0.76 | 0.621 | $2.4 \times 10^2$ | 0.82 | 0.49 |

KGE: Kling-Gupta efficiency.

## 6. Conclusion

In this study, the hydrological modeling of the Ganga watershed was performed successfully using the SWAT. A significant outcome was obtained using 20 years of daily meteorological data from 1996 to 2015. The period from 2000 to 2004 was used as a warm-up period, and the results of the period from 2004 to 2015 were divided into two halves. The first half, from 2004 to 2009, was used for calibration, and the second half, from 2009 to 2015, was used for validation. The calibration was done using the three algorithms of GLUE, SUFI-2, and ParaSol; the results were used to compare these algorithms. The comparison showed that of the three calibration algorithms, SUFI-2 performed the best, as it accounted better for uncertainties and required the smallest number of computational parameters for calibration. The main limitations of SUFI-2 are as follows: ① Without good knowledge of the parameters' effects on the stream flow and soil erosion, running SUFI-2 may become difficult for the user; and ② SUFI-2 does not consider parameter correlations, which decreases its ability.

The results obtained after calibration and validation using SUFI-2 were the monthly outcome values of $R^2 = 0.78$ and NSE = 0.76 for the calibration period. We obtained the values of $R^2 = 0.71$ and NSE = 0.756 for the validation time frame. The affectability examination of the SWAT on the sub-watershed delineation and HRU definition thresholds demonstrated that the stream was more sensitive to the HRU definition thresholds than to the sub-watershed discretization. The outcomes in this watershed were 760 HRUs throughout the basin. The 95PPU sections corresponded very well with the observed information in the calibration and validation time frames. The P-factor and R-factor calculated with SUFI-2 yielded excellent outcomes, by bracketing value higher than 75% of the observed data. SUFI-2 calculation was therefore considered to be a viable strategy, although it requires extra emphasis and an additional requirement for changing parameter ranges. Despite information uncertainty, the SWAT model creates excellent reproduction consequences for monthly time steps, which are helpful for water resource management in this watershed.

## Acknowledgements

## Compliance with ethics guidelines

Nikita Shivhare, Prabhat Kumar Singh Dikshit, and Shyam Bihari Dwivedi declare that they have no conflict of interest or financial conflicts to disclose.

## References

[1] Kumar S, Mishra A, Raghuwanshi NS. Identification of critical erosion watersheds for control management in data scarce condition using the SWAT model. J Hydrol Eng 2015;20(6):C4014008.
[2] Khalid K, Ali MF, Rahman NFA, Mispan MR, Haron SH, Othman Z, et al. Sensitivity analysis in watershed model using SUFI-2 algorithm. Procedia Eng 2016;162:441–7.
[3] Salimi ET, Nohegar A, Malekian A, Hosseini M, Holisaz A. Runoff simulation using SWAT model and SUFI-2 algorithm (case study: Shafaroud watershed, Guilan Province, Iran). Caspian J Environ Sci 2016;14:69–80.
[4] Noori N, Kalin L. Coupling SWAT and ANN models for enhanced daily streamflow prediction. J Hydrol 2016;533:141–51.
[5] Qiu Z, Wang L. Hydrological and water quality assessment in a suburban watershed with mixed land uses using the SWAT model. J Hydrol Eng 2014;19(4):816–27.
[6] Pisinaras V, Petalas C, Gikas GD, Gemitzi A, Tsihrintzis VA. Hydrological and water quality modeling in a medium-sized basin using the Soil and Water Assessment Tool (SWAT). Desalination 2010;250(1):274–86.
[7] Omani N, Tajrishy M, Abrishamchi A. Modeling of a river basin using SWAT model and SUFI-2. Proceedings of the 4th International SWAT Conference, 2007.
[8] Fukunaga DC, Cecílio RA, Zanetti SS, Oliveira LT, Caiado MAC. Application of the SWAT hydrologic model to a tropical watershed at Brazil. Catena 2015;125:206–13.
[9] Shi P, Hou Y, Xie Y, Chen C, Chen X, Li Q, et al. Application of a SWAT model for hydrological modeling in the Xixian Watershed, China. J Hydrol Eng 2013;18(11):1522–9.
[10] Briak H, Moussadek R, Aboumaria K, Mrabet R. Assessing sediment yield in Kalaya gauged watershed (Northern Morocco) using GIS and SWAT model. Int Soil Water Conserv Res 2016;4(3):177–85.
[11] Jeong J, Kannan N, Arnold JG, Glick R, Gosselink L, Srinivasan R, et al. Modeling sedimentation-filtration basins for urban watersheds using soil and water assessment tool. J Environ Eng 2013;139(6):838–48.
[12] Yesuf HM, Assen M, Alamirew T, Melesse AM. Modeling of sediment yield in Maybar gauged watershed using SWAT, northeast Ethiopia. Catena 2015;127:191–205.
[13] Vigiak O, Malagó A, Bouraoui F, Vanmaercke M, Obreja F, Poesen J, et al. Modelling sediment fluxes in the Danube River Basin with SWAT. Sci Total Environ 2017;599–600:992–1012.
[14] Sardar B, Singh AK, Raghuwanshi NS, Chatterjee C. Hydrological modeling to identify and manage critical erosion-prone areas for improving reservoir life: case study of Barakar Basin. J Hydrol Eng 2014;19(1):196–204.
[15] Psomas A, Panagopoulos Y, Konsta D, Mimikou M. Designing water efficiency measures in a catchment in Greece using WEAP and SWAT models. Procedia Eng 2016;162:269–76.
[16] Vigiak O, Malagó A, Bouraoui F, Vanmaercke M, Poesen J. Adapting SWAT hillslope erosion model to predict sediment concentrations and yields in large basins. Sci Total Environ 2015;538:855–75.
[17] Vilaysane B, Takara K, Luo P, Akkharath I, Duan W. Hydrological stream flow modelling for calibration and uncertainty analysis using SWAT model in the Xedone River Basin, Lao PDR. Procedia Environ Sci 2015;28:380–90.
[18] Ercan MB, Goodall JL, Castronova AM, Humphrey M, Beekwilder N. Calibration of SWAT models using the cloud. Environ Model Softw 2014;62:188–96.
[19] Talebizadeh M, Morid S, Ayyoubzadeh SA, Ghasemzadeh M. Uncertainty analysis in sediment load modeling using ANN and SWAT Model. Water Resour Manage 2010;24(9):1747–61.
[20] Zhang X, Srinivasan R, Bosch D. Calibration and uncertainty analysis of the SWAT model using Genetic Algorithms and Bayesian Model Averaging. J Hydrol 2009;374(3–4):307–17.
[21] Tuo Y, Duan Z, Disse M, Chiogna G. Evaluation of precipitation input for SWAT modeling in Alpine catchment: a case study in the Adige River Basin (Italy). Sci Total Environ 2016;573:66–82.
[22] Zhang X, Srinivasan R, Van Liew M. Approximating SWAT model using artificial neural network and support vector machine 1. J Am Water Resour Assoc 2009;45(2):460–74.
[23] Romagnoli M, Portapila M, Rigalli A, Maydana G, Burgués M, García CM. Assessment of the SWAT model to simulate a watershed with limited available data in the Pampas region. Argentina. Sci Total Environ 2017;596–597:437–50.
[24] Neitsch SL, Arnold JG, Kiniry JR, Williams JR. Soil and water assessment tool. Theoretical documentation version 2009. Report. College Station: Texas Water Resources Institute, Texas A&M University System; 2011. Report No.:406.
[25] Abbaspour KC. Calibration and uncertainty programs—a user manual. Proceedings of the SWAT-CUP Workshop. Dübendorf: Swiss Federal Institute of Aquatic Science and Technology (Eawag); 2014.
[26] Arnold JG, Moriasi DN, Gassman PW, Abbaspour KC, White MJ, Srinivasan R, et al. SWAT: model use, calibration, and validation. Trans ASABE 2012;55:1491–508.